Check for updates

The Relevance of Forest Structure for Biomass and Productivity in Temperate Forests: New Perspectives for Remote Sensing

Rico Fischer, et al. *[full author details at the end of the article]*

Abstract

Forests provide important ecosystem services such as carbon sequestration. Forest land-scapes are intrinsically heterogeneous—a problem for biomass and productivity assessment using remote sensing. Forest structure constitutes valuable additional information for the improved estimation of these variables. However, survey of forest structure by remote sensing remains a challenge which results mainly from the differences in forest structure metrics derived by using remote sensing compared to classical structural metrics from field data. To understand these differences, remote sensing measurements were linked with an individual-based forest model. Forest structure was analyzed by lidar remote sensing using metrics for the horizontal and vertical structures. To investigate the role of forest structure for biomass and productivity estimations in temperate forests, 25 lidar metrics of 375,000 simulated forest stands were analyzed. For the lidar-based metrics, top-of-canopy height arose as the best predictor for describing horizontal forest structure. The standard deviation of the vertical foliage profile was the best predictor for the vertical heterogeneity of a forest. Forest structure was also an important factor for the determination of forest biomass and aboveground wood productivity. In particular, horizontal structure was essential for forest biomass estimation. Predicting aboveground wood productivity must take into account both horizontal and vertical structures. In a case study based on these findings, forest structure, biomass and aboveground wood productivity are mapped for whole of Germany. The dominant type of forest in Germany is dense but less vertically structured forest stands. The total biomass of all German forests is 2.3 Gt, and the total aboveground woody productivity is 43 Mt/year. Future remote sensing missions will have the capability to provide information on forest structure (e.g., from lidar or radar). This will lead to more accurate assessments of forest biomass and productivity. These estimations can be used to evaluate forest ecosystems related to climate regulation and biodiversity protection.

---

1 Introduction

Forests are crucial components of the Earth system. They represent an important pool in the global carbon cycle as they bind huge amounts of atmospheric carbon (Bonan 2008; Grace et al. 2014; Pan et al. 2011). Quantifying forest carbon stocks (e.g., forest biomass) and forest carbon fluxes (e.g., forest productivity) is important for understanding the effects of land use and climate change (Foley et al. 2005). However, forests can be heterogeneously structured which lead to variable biomass stocks and carbon fluxes (Rödig et al. 2018; Saatchi et al. 2011). The structural heterogeneity makes it difficult to reliably estimate forest biomass or forest productivity for larger regions. For example, biomass estimations for the Amazon rainforest—the largest intact tropical forest on Earth—range from 39 to 93 GtC (Houghton et al. 2001; Malhi et al. 2006; Saatchi et al. 2007, 2011). The range of estimates arises from different methodological approaches which take into account the landscape heterogeneity in different ways.

Remote sensing is a promising technique that can be used to capture the state of forests with high spatial resolution (e.g., Exbrayat et al. 2019). However, remote sensing cannot measure directly forest biomass and productivity, but it can partly detect the structure of forests. In general, forest structure is related to the spatial distribution of trees and their variability in size (Schall et al. 2018b). Most of current estimates of forest biomass from remote sensing are based on relationships between forest structure and biomass. Forest height characterizes one aspect of forest structure. For example, forest canopy height, derived from lidar remote sensing, is often used for forest biomass estimations (Asner and Mascaro 2014; Dubayah et al. 2010; Lefsky et al. 1999). However, more complex structural characteristics of forests are often ignored, and considerable uncertainties remain.

Forest structure, however, is an important element in forest ecology as it is linked to many ecological processes (Pretzsch 2009; Shugart et al. 2010; Snyder 2010). It is also used as indicator for biodiversity, as vertically structured forests foster the biodiversity of some taxa (Boncina 2000; Ishii et al. 2004; Schall et al. 2018a). Further, horizontal and vertical structural heterogeneities enhance resistance of forest ecosystems against disturbances (Dobbertin 2002; Pretzsch et al. 2016). Some studies also explored the effects of forest structure on forest productivity (Bohn and Huth 2017; Dănescu et al. 2016; Hardiman et al. 2011; Liang et al. 2016; Schall et al. 2018b) and found that variables characterizing forest structure are the main drivers of forest productivity instead of biodiversity variables.

Although forest structure plays an important role in understanding forest dynamics, there are no global forest structure maps available. There are few coarse-resolution maps, but these only show components of forest structure (e.g., forest height from MODIS and ICESat, resolution 1 km; Lefsky 2010; Simard et al. 2011). Clearly, an efficient analysis of the multilayered forest structure for larger regions is required. New satellite missions are being launched (e.g., GEDI, BIOMASS and Tandem-L) which will use novel technologies to measure forest structure on a global scale including forest height and vertical heterogeneity.

A systematic framework for ecologically meaningful structural classes has been recently proposed, which suggests two main elements: the horizontal and the vertical forest structures (Bohn and Huth 2017; Cazcarra-Bes et al. 2017; Fischer et al. 2019; Tello et al. 2014, 2018). However, there are several ways to describe horizontal and vertical forest structures from field data (del Río et al. 2016; Pommerening 2002; Reineke 1933; Shugart 2003; Zenner and Hibbs 2000). It will be difficult to find a suitable definition of forest structure

for a wide range of applications, spatial scales and forest types. Moreover, forest structure metrics are different depending on whether they are based on field or remote sensing data. Field-based descriptors for forest structure are derived from individual tree size measurements, while remote sensing descriptors are often based on the heterogeneous canopy structure for a given area (Cazcarra-Bes et al. 2017). A hybrid approach for forest structure measured by field data and by remote sensing is the terrestrial laser scanning, which allows very detailed measurements of single trees and forest canopy structure (Disney 2018). However, this technique is limited to forest with a limited extent due to its high degree of detail. Airborne or satellite-based remote sensing data are therefore a suitable choice for capturing forest structure on a larger scale.

In this study, we combined forest inventory data, forest modeling and airborne lidar remote sensing to answer the question, "How can we estimate forest structure from remote sensing, and what is the role of forest structure for forest biomass and aboveground wood productivity estimations?" The aim is to classify forests into structural categories, using horizontal and vertical structural descriptors that can be measured by remote sensing (Fig. 1). Based on this structural classification, we explore whether forest biomass and aboveground wood productivity can be estimated more accurately if structural information is included. We are using an individual-based model to generate hypotheses on the relations among structural variables and ecosystem variables (aboveground wood productivity and biomass). Since the output from individual-based forest models (a tabulation of each tree, its species and its size) resembles standard forest inventories from field data, obtained results can be directly applied to forest inventories.

We used the forest model FORMIND (Bohn and Huth 2017; Fischer et al. 2016) to generate thousands of forest stands. With this large set of data, we examined in detail the role of forest structure for biomass and aboveground wood productivity estimations. Furthermore, in a case study for Germany we will explore how well forest biomass and aboveground wood productivity can be derived from remote sensing data including information

Fig. 1 Biomass and aboveground wood productivity estimations are related to forest structure. In this study, we distinguish between horizontal forest structure, which represents the density of trees in a forest stand, and the vertical forest structure, which quantifies the vertical heterogeneity of tree heights. Forest structure can be estimated by measurements from field data and from remote sensing
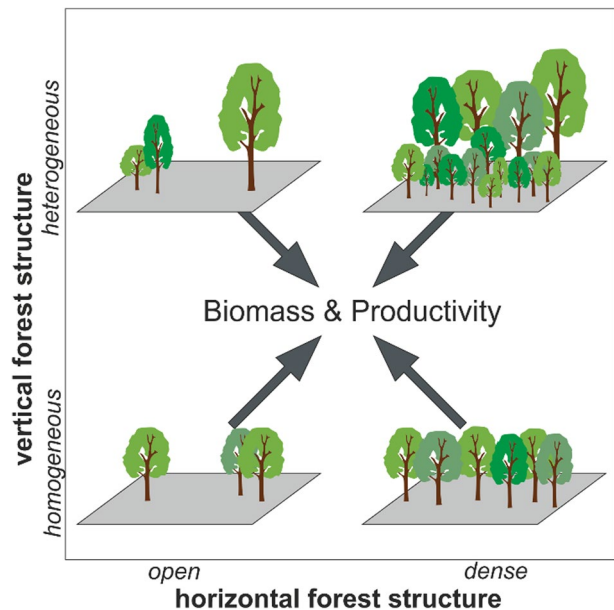
on forest structure (Fig. 2). This presents a conceptual approach that can be applied across large areas where lidar data are available.

2 Methods

2.1 Simulating Temperate Forest Stands with a Forest Model

We applied the individual- and process-based forest gap model FORMIND (Fischer et al. 2016) in the "forest factory mode." In contrast to classical long-term simulations, this mode allows the creation of thousands of forest stands based on different stem size distributions and species mixtures. For each forest stand, competitions for light, space and water were calculated depending on the spatial arrangement and the size of the trees (by applying established processes from the FORMIND model). A full forest inventory is then available for each stand, which can include different arrangements of trees leading to different horizontal and vertical structures.

In order to generate such forest stands, trees were randomly selected from the stem size distribution, were given a species identity and were then planted within a stand. Fifteen stem size distributions were applied, which cover a gradient from young to old and disturbed to undisturbed forests (tree height differ between 5 m and 40 m). Species mixtures
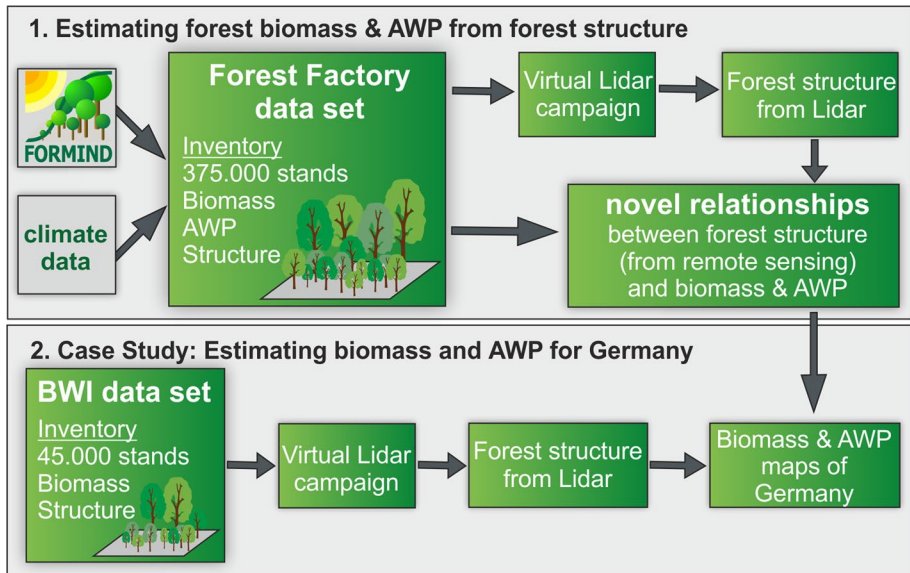
Fig. 2 Concept of this study. (1) Applying the forest model FORMIND, a large data set of virtual forest stands was generated ("forest factory data set"). For each forest stand of this data set, a virtual lidar campaign was simulated. These lidar data were used to estimate forest structure from remote sensing data. Then, relationships were explored to determine aboveground biomass and aboveground woody productivity (AWP) using remote sensing-based forest structure metrics. (2) In a case study for Germany, a lidar campaign was simulated for each forest stand from the national forest inventory data set of Germany (BWI). Forest structure for each stand was estimated from this lidar data. Based on the estimated forest structure and the relationships found in the first part of this study, Germany-wide maps of biomass and AWP were produced

included all combinations of eight common temperate species using the species-specific allometries and model algorithms of the FORMIND model version for temperate forests (Bohn et al. 2014). For each combination of age and species, we assembled 100 simulated forest stands, each stand with a size of 20 m×20 m. This is done under the conditions that: (1) there is enough space available for the crowns of every tree and (2) every tree in the simulated forest has positive net primary productivity under environmental conditions of the temperate zone (light, temperature, water). The net primary productivity of each forest in this study is calculated using climate date of a site in Germany (climate station of the Hainich, Germany). In total, five different climates over time were applied (years 2000–2004). For more details regarding the forest factory mode of the FORMIND model, see Bohn and Huth (2017).

In this "forest factory mode," we have created a total of 375,000 different virtual forest stands, each characterized by an inventory of all trees. We refer always to this data set if the term "field data" is used within this study. For each stand, the simulated forest structure was described by horizontal and vertical structural characteristics (e.g., basal area, maximal tree height). In addition, aboveground biomass (AGB) and aboveground woody productivity (AWP) of each forest stand were calculated using the FORMIND model. The full data set is available in Electronic supplementary material.

2.2 Remote Sensing Data

For each forest stand, a lidar point cloud was simulated following the approach described by Knapp et al. (2018a). This lidar model uses the positions, heights, crown diameters and crown lengths of all trees to generate a 3D voxel representation of a stand and to simulate lidar measurements. The point clouds obtained for all stands were rasterized to 1 m resolution canopy height models (CHM) by taking the height values of the highest returns in each 1 m pixel, respectively, and setting empty pixels to ground height 0. Data were further aggregated to vertical CHM profiles of 1-m height bins which served as inputs to calculate vertical foliage profiles (VFP, see section "Describing forest structure from field data" of Appendix 1).

2.3 Describing Forest Structure with Field Data and Lidar Remote Sensing

Several structural indices were used to characterize the forest structure. For each 20 m×20 m forest stand from the forest factory data set, we calculated horizontal and vertical descriptors of the structure from field data and from remote sensing data. Here, we present the most important metrics used in this study. However, other metrics are also possible. In total, 13 metrics were examined to describe forest structure from field data and 25 metrics which estimate forest structure from lidar remote sensing. A full list of all these indices can be found in sections "Describing forest structure from field data" and "Describing forest structure from remote sensing data" of Appendix 1.

2.3.1 Forest Structure Estimation from Field Data

Forest structure can be described by metrics derived from tree-level inventory data—from either real forest inventories or simulated stands. Here, these descriptors of forest structure were inspired by previous studies (Bohn and Huth 2017; Cazcarra-Bes et al.

2017; Fischer et al. 2019). Horizontal structure is described by stand basal area BA (m^2), which is the sum of all tree basal area values of one forest stand:

$$\mathrm{BA} = \sum_{\text{trees}} \frac{\pi}{4} d^2,$$

where d (m) is the stem diameter of a tree. Vertical structure is quantified by the standard deviation of tree heights $\mathrm{SD_{th}}$ (m):

$$\mathrm{SD_{th}} = \sqrt{\frac{1}{n-1} \sum_{\text{trees}} \left(h - \bar{h}\right)^2},$$

where h (m) is the height of a tree and $\bar{h}$ (m) the mean tree height of a stand.

2.3.2 Forest Structure Estimation from Remote Sensing

Horizontal structure for each forest stand from the lidar data set is described by the mean top-of-canopy height (m), which is the mean of the canopy height model (CHM) with 1 m resolution:

$$\mathrm{TCH} = \frac{\sum_{i=1}^{i\max} P_{\mathrm{CHM},i}}{i_{\max}},$$

where $P_{\mathrm{CHM},i}$ is the height of the CHM in pixel i and $i_{\max}$ is the total number of pixels. Vertical structure is quantified by the standard deviation of the vertical foliage profile ($\mathrm{SD_{VFP}}$ (m)):

$$\mathrm{SD_{VFP}} = \sqrt{\frac{\sum_{i=1}^{i\max} \left(p_i \cdot \left(h_i - \frac{\sum_{i=1}^{i\max} (p_i \cdot h_i)}{\sum_{i=1}^{i\max} p_i} \right)^2 \right)}{\frac{N-1}{N} \cdot \sum_{i=1}^{i\max} p_i}},$$

where p_i is the foliage profile value (leaf area per m^2) in height bin h_i, $i_{\max}$ is the number of height bins and N is the count of all p_i that are not zero. The process of creating the required vertical foliage profile (VFP) from a discrete lidar point cloud is described in section "Calculating the vertical foliage profile from a CHM" of Appendix 1.

2.4 Estimating Forest Biomass and Productivity from Forest Structure

For estimating forest biomass and aboveground wood productivity, we follow a two-step approach. First, horizontal (i.e., TCH) and vertical (i.e., $\mathrm{SD_{VFP}}$) forest structure was estimated based on remote sensing measurements. Second, the derived information on forest structure was used to estimate forest biomass and aboveground wood productivity. We compare three different approaches which differ in the degree of complexity:

(a) H_{struct}: We estimate the aboveground biomass (AGB) and aboveground woody productivity (AWP) only with the information from the horizontal forest structure (here TCH). For this, we used the following power-law approach:

$$\text{AGB}_H = a \cdot \text{TCH}^b, \text{AWP}_H = m \cdot \text{TCH}^n.$$

(b) V_{struct}: We estimate the biomass and productivity only from the vertical forest structure (here SD_{VFP}).

$$\text{AGB}_V = a \cdot \text{SD}_{\text{VFP}}^b, \text{AWP}_H = m \cdot \text{SD}_{\text{VFP}}^p.$$

(c) $H_{\text{struct}} + V_{\text{struct}}$: We estimate the biomass and productivity from the horizontal and vertical forest structures.

$$\text{AGB}_{H+V} = a \cdot \text{TCH}^b \cdot \text{SD}_{\text{VFP}}^p, \text{AWP}_{H+V} = m \cdot \text{TCH}^n \cdot \text{SD}_{\text{VFP}}^p.$$

For all three variants, we applied the artificial forest stand data set described in Sect. 2.1. For each simulated forest stand, a virtual 3D airborne lidar scan was available (Sect. 2.2). Using these lidar data, for each stand all structural metrics (e.g., TCH, SD_{VFP}) were calculated (Sect. 2.3). Beside these metrics, also AGB and AWP are known for all stands. With this information, we fitted the unknown parameters of equations (a)–(c) by linear model fit using the double logarithmic transformation.

2.5 Preparation of Nationwide Biomass and Productivity Maps with the German National Forest Inventory Data Set

The German national forest inventory data (BWI) record forest stands on a sample basis according to a standardized procedure throughout Germany (Thuenen-Institut 2015). It consists of more than 45,000 field plots and is repeated every 10 years. The field plot varies in size (circa 20 m×20 m) due to the angle count sampling method. For every plot of the BWI data set, the stem diameter (DBH) and species identification of all trees measured were available. Tree height and aboveground biomass were calculated using the same species-specific allometries as applied to the forest factory data set (Sect. 2.1). The BWI plots are distributed on a regular grid across Germany. Plot density varies between regions but there is at least one plot located within each 4 km×4 km grid cell. For each forest stand of the BWI, all structural and stand features were determined as described above (cf. section "Describing forest structure from field data" of Appendix 1), a virtual lidar campaign was carried out and the remote sensing-based metrics were then calculated (cf. section "Describing forest structure from remote sensing data" of Appendix 1).

Using the information on forest structure from simulated lidar remote sensing for each BWI plot and the equations from Sect. 2.4 (parameters are derived from the forest factory data set), we derived forest biomass and aboveground wood productivity maps for Germany. As the exact positions of the BWI plots are unknown, we used their approximate positions (on the regular grid, i.e., with a precision of at least 4 km) to geolocate the estimated forest attributes for each plot. We used Voronoi tessellation to interpolate between BWI plots. In this procedure, each forested point in Germany got assigned to the closest BWI plot nearby. Gridded maps of the different forest attributes were produced by rasterizing the tessels with 250 m pixel resolution. The rasters were masked with a forest cover mask based on a forest cover map from Hansen et al. (2013; 50% minimum tree cover, resampled to 250 m resolution).

3 Results

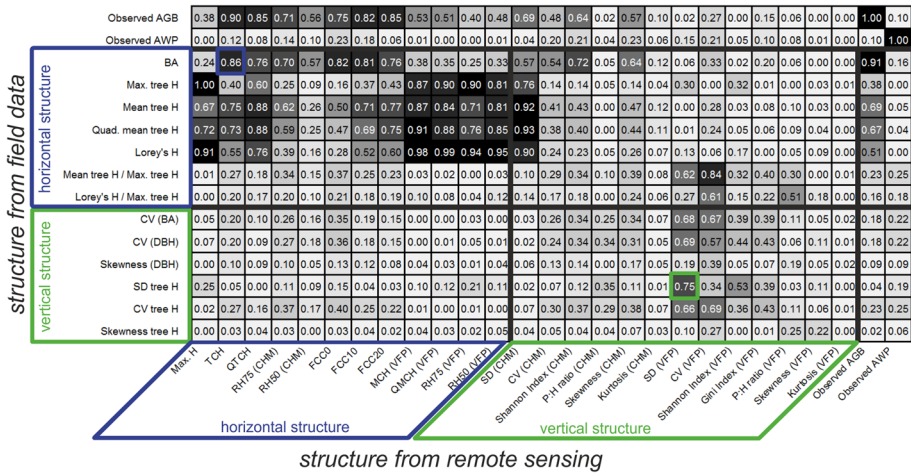## 3.1 Estimating Forest Structure from Lidar Remote Sensing

Analyzing 375,000 forest stands from the forest factory data set, we investigated whether forest structure can be determined using lidar remote sensing. For this purpose, two field-based metrics were analyzed—basal area (BA) as proxy for the horizontal forest structure (i.e., the density of the forest) and tree height heterogeneity (SD_{th}) as proxy for the vertical heterogeneity of a forest stand. In total, we tested 325 correlations between structural descriptors estimated from field data and remote sensing data. Top-of-canopy height (TCH) as a horizontal descriptor estimated from remote sensing has the highest correlation with the horizontal metric basal area estimated from field data ($r^2 = 0.86$, see Fig. 3a). The quadratic top-of-canopy height ($r^2 = 0.76$, see Fig. 4) and the fractional canopy cover with a threshold of 10 m ($r^2 = 0.81$) show similar results and are also suitable to estimate the horizontal structure.

For the vertical forest structure, the standard deviation of the vertical foliage profile (SD_{VFP}) shows the strongest correlation with the field-based metric SD_{th} ($r^2 = 0.75$, see Fig. 3b). The Shannon index of the vertical foliage profile also reveals a relevant correlation ($r^2 = 0.53$, see Fig. 4), but the analysis did not identify any further remote sensing metric that could be used to describe the vertical structure. A full list of all analyzed correlations between field-based structural metrics and remote sensing-based metrics is shown in Fig. 4. For the analyses that follow, the remote sensing-based metrics with the highest correlation were used, i.e., TCH as proxy for the horizontal structure and SD_{VFP} as proxy for the vertical structure.

(a) horizontal structure   **(b)** vertical structure
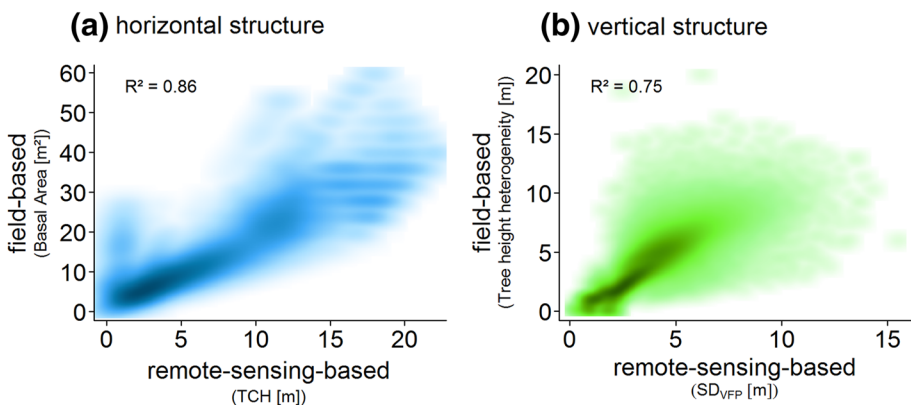
Fig. 3 Remote sensing-based estimation of the forest structure based on the analysis of the forest factory data set. The figure shows the estimate of **a** the horizontal forest structure (basal area) using top-of-canopy height (TCH) derived from lidar and **b** the estimate of the vertical forest structure (tree height heterogeneity) using the standard deviation of the vertical foliage profile (SD_{VFP}) derived also from lidar. For this study, all forest inventories from the forest factory data set (in total 375,000 temperate forest stands with a size of 20 m × 20 m) were analyzed

structure from field data — horizontal structure / vertical structure

	Max. H	TCH	QTCH	RH75 (CHM)	RH50 (CHM)	FCC0	FCC10	FCC20	MCH (VFP)	QMCH (VFP)	RH75 (VFP)	RH50 (VFP)	SD (CHM)	CV (CHM)	Shannon Index (CHM)	P:H ratio (CHM)	Skewness (CHM)	Kurtosis (CHM)	SD (VFP)	CV (VFP)	Shannon Index (VFP)	Gini Index (VFP)	P:H ratio (VFP)	Skewness (VFP)	Kurtosis (VFP)	Observed AGB	Observed AWP
Observed AGB	0.38	0.90	0.85	0.71	0.56	0.75	0.82	0.85	0.53	0.51	0.40	0.48	0.69	0.48	0.64	0.02	0.57	0.10	0.02	0.27	0.00	0.15	0.06	0.00	0.00	1.00	0.10
Observed AWP	0.00	0.12	0.08	0.14	0.10	0.23	0.18	0.06	0.01	0.00	0.00	0.01	0.04	0.20	0.21	0.04	0.23	0.06	0.15	0.21	0.05	0.10	0.08	0.01	0.00	0.10	1.00
BA	0.24	0.86	0.76	0.70	0.57	0.82	0.81	0.76	0.38	0.35	0.25	0.33	0.57	0.54	0.72	0.05	0.64	0.12	0.06	0.33	0.02	0.20	0.06	0.00	0.00	0.91	0.16
Max. tree H	1.00	0.40	0.60	0.25	0.09	0.16	0.37	0.43	0.87	0.90	0.90	0.81	0.76	0.14	0.14	0.05	0.14	0.04	0.30	0.00	0.32	0.01	0.00	0.03	0.01	0.38	0.00
Mean tree H	0.67	0.75	0.88	0.62	0.26	0.50	0.71	0.77	0.87	0.81	0.92	0.41	0.43	0.00	0.47	0.12	0.00	0.28	0.03	0.08	0.10	0.03	0.00	0.00	0.00	0.69	0.05
Quad. mean tree H	0.72	0.55	0.88	0.59	0.25	0.47	0.69	0.75	0.91	0.88	0.76	0.85	0.93	0.38	0.40	0.00	0.44	0.11	0.01	0.24	0.05	0.06	0.09	0.04	0.00	0.67	0.04
Lorey's H	0.91	0.53	0.76	0.39	0.16	0.28	0.52	0.60	0.98	0.99	0.94	0.95	0.90	0.24	0.23	0.05	0.26	0.07	0.13	0.06	0.17	0.00	0.05	0.09	0.00	0.51	0.00
Mean tree H / Max. tree H	0.01	0.27	0.18	0.34	0.15	0.37	0.25	0.23	0.03	0.02	0.00	0.03	0.10	0.29	0.34	0.10	0.39	0.08	0.62	0.84	0.32	0.40	0.30	0.00	0.01	0.23	0.25
Lorey's H / Max. tree H	0.00	0.20	0.17	0.20	0.10	0.21	0.18	0.19	0.10	0.08	0.04	0.12	0.14	0.17	0.18	0.00	0.24	0.06	0.27	0.61	0.15	0.22	0.51	0.18	0.00	0.16	0.18
CV (BA)	0.05	0.20	0.10	0.26	0.16	0.35	0.19	0.15	0.00	0.00	0.03	0.00	0.03	0.02	0.24	0.35	0.34	0.07	0.68	0.67	0.39	0.39	0.11	0.05	0.02	0.18	0.22
CV (DBH)	0.07	0.20	0.09	0.27	0.18	0.36	0.18	0.15	0.00	0.01	0.04	0.02	0.24	0.34	0.34	0.31	0.05	0.69	0.57	0.44	0.43	0.06	0.11	0.01	0.02	0.18	0.22
Skewness (DBH)	0.00	0.10	0.09	0.10	0.05	0.13	0.12	0.08	0.04	0.03	0.01	0.04	0.06	0.13	0.14	0.00	0.17	0.05	0.19	0.39	0.05	0.07	0.19	0.05	0.02	0.09	0.09
SD tree H	0.25	0.05	0.00	0.11	0.09	0.15	0.04	0.03	0.10	0.12	0.21	0.11	0.02	0.07	0.12	0.35	0.11	0.01	0.75	0.34	0.53	0.39	0.03	0.11	0.00	0.04	0.19
CV tree H	0.02	0.27	0.16	0.37	0.17	0.40	0.25	0.22	0.01	0.00	0.03	0.02	0.04	0.07	0.30	0.37	0.29	0.38	0.07	0.66	0.69	0.36	0.43	0.11	0.06	0.23	0.25
Skewness tree H	0.00	0.03	0.04	0.03	0.00	0.03	0.04	0.02	0.04	0.03	0.02	0.05	0.04	0.05	0.04	0.04	0.03	0.00	0.10	0.27	0.00	0.10	0.25	0.22	0.00	0.06	0.06

horizontal structure — vertical structure — **structure from remote sensing**

Fig. 4 Correlations (coefficient of determination r^2) between field-based structural metrics and remote sensing-based metrics. Numbers and gray scale indicate the coefficient of determination. For each of the 375 correlations, in total 375,000 forest stands from the forest factory data set (Sect. 2.1) were analyzed. For every virtual forest stand, a forest inventory was available allowing the calculation of the aboveground biomass (AGB) and several structural indices (e.g., maximum tree height, standard deviation of tree height). The productivity AWP for each stand was determined by applying the FORMIND model. All structural indices from remote sensing are derived from the virtual lidar campaign for each forest stand in the forest factory data set. Highlighted are the two correlations from Fig. 3 for the horizontal structure (blue) and vertical structure (green). All structural metrics are explained in section "Describing forest structure from field data" of Appendix 1 (field-based) and "Describing forest structure from remote sensing data" of Appendix 1 (remote sensing-based)

3.2 Analyzing the Role of Remote Sensing-Based Forest Structure for Biomass and Productivity Estimations

All 375,000 temperate forest stands from the forest factory data set were analyzed to investigate the role of forest structure for the determination of forest biomass and aboveground wood productivity. For this purpose, the forest stands were grouped into sixteen forest structure classes with equal spacing, consisting of four horizontal (TCH 0–6 m, 6–12, 12–18, > 18) and four vertical (SD_{VFP} 0–2 m, 2–4, 4–6, > 6) structure classes. It turns out that forest structure is a key factor in estimating forest biomass and aboveground wood productivity. There is an increase in forest biomass with increasing TCH—which is a proxy for the horizontal structure (Fig. 5a). However, biomass in forests with an open horizontal structure (TCH < 12 m) is much more influenced by vertical structure than in closed forests (TCH > 12 m).

The relation between aboveground wood productivity and forest structure is more complex. For stands with a homogeneous vertical structure (SD_{VFP} between 0 and 2 m), the productivity increases with the density of the forest (high horizontal structure; Fig. 5b). The highest productivity is achieved for these single-layer forest stands ($SD_{VFP} < 2$ m) and a medium dense horizontal structure (TCH around 15 m). However, as the vertical structure increases to more heterogeneous stands ($SD_{VFP} > 2$ m), the positive effect of the horizontal forest structure on productivity is reduced. For forest stands with heterogeneous vertical structure ($SD_{VFP} > 4$ m), productivity increases only slightly with increasing density
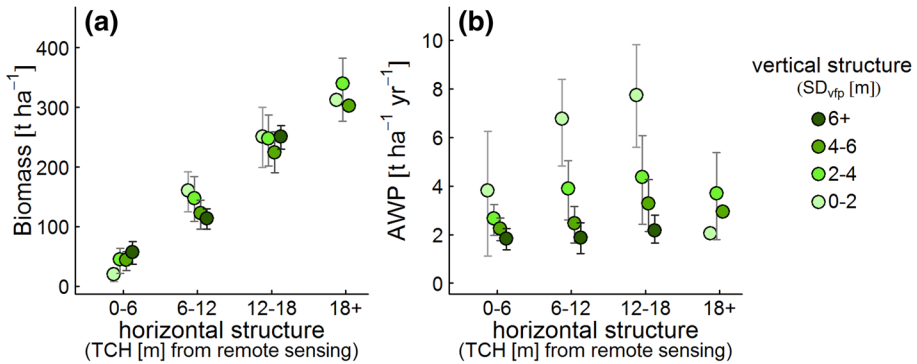
Fig. 5 Role of forest structure for biomass and aboveground wood productivity (AWP) estimations. For all 375,000 forest stands, forest structure was estimated from remote sensing. As horizontal forest structure descriptor, the top-of-canopy height (TCH) was used, and as vertical structure descriptor, the standard deviation of the vertical foliage profile (SD_{VFP}) was used. All forest stands were grouped in 16 structure classes (four horizontal classes and four vertical classes). Shown are **a** the observed mean aboveground biomass and **b** the observed mean aboveground wood productivity (AWP) in relation to the forest structure classes. Biomass and AWP values are taken directly from the forest factory data set. Error bars indicate the standard deviation

of the horizontal structure and can even decline for forests with dense horizontal structure (TCH > 18 m). Forests with a heterogeneous vertical structure represent multilayered forests where large trees shade smaller trees, which then reduce the aboveground wood productivity of smaller trees. To summarize, following the analysis of 375,000 forest stands from the forest factory data set TCH (as a proxy for the horizontal forest structure) plays an important role in forest state monitoring (like forest biomass). However, both horizontal and vertical forest structures are relevant for aboveground wood productivity estimates (Fig. 5b; Table 1).

To quantify the relation between forest structure and biomass/productivity, three statistical approaches between these variables were investigated (cf., methods 2.4). On the one hand, these approaches were created with only one information about forest structure and on the other hand with information on horizontal and vertical forest structures (Table 1).

Table 1 Aboveground biomass (AGB) and aboveground wood productivity (AWP) determined using structural metrics from 3D remote sensing (TCH as horizontal descriptor, SD_{VFP} as vertical descriptor)

Approach	Forest biomass AGB (t/ha)	Forest productivity AWP [t/(ha year)]
H_{struct}	$AGB_H = 9.49 \cdot TCH^{1.22}$ $r^2 = 0.90$, rmse $= 28\,(30\%)$	$AWP_H = 1.68 \cdot TCH^{0.31}$ $r^2 = 0.14$, rmse $= 2.1\,(75\%)$
V_{struct}	$AGB_V = 34.77 \cdot SD_{VFP}^{0.48}$ $r^2 = 0.01$, rmse $= 98\,(158\%)$	$AWP_V = 4.03 \cdot SD_{VFP}^{-0.34}$ $r^2 = 0.09$, rmse $= 2.1\,(75\%)$
$H_{struct} + V_{struct}$	$AGB_{H+V} = 7.55 \cdot TCH^{1.20} \cdot SD_{VFP}^{0.23}$ $r^2 = 0.90$, rmse $= 29\,(31\%)$	$AWP_{H+V} = 2.55 \cdot TCH^{0.34} \cdot SD_{VFP}^{-0.39}$ $r^2 = 0.31$, rmse $= 1.8\,(64\%)$

For the calibration of the approaches, all forest stands (20 m × 20 m) from the forest factory data set were used. R-squared values indicate the correlation between observed value from the forest factory data set and the estimated value using the corresponding approach. For all approaches we got a p value ≤ 0.01. Given are the root-mean-square error (RMSE) and the normalized RMSE (nRMSE; normalized by the mean value of the observation). The detailed scatterplots can be found in Appendix 1 (Figs. 9 and 10)

The best results for biomass estimation are obtained with the H_{struct} and $H_{\text{struct}} + V_{\text{struct}}$ approach ($r^2 = 0.90$, nRMSE = 30%; Table 1 and Fig. 9), while only the $H_{\text{struct}} + V_{\text{struct}}$ approach is somehow suitable for aboveground wood productivity estimation ($r^2 = 0.31$, nRMSE = 64%; Table 1 and Fig. 10). The error for the productivity estimate for forest stands with a size of 20 m × 20 m can be improved from 75 to 64% by taking both structural dimensions into account (Fig. 6; Table 1).

3.3 Case Study: Estimating Forest Biomass and Productivity at Country Level

We estimate forest structure for whole of Germany based on 45,000 plots from the German national forest inventory data (BWI data set) and relate this information to forest biomass and aboveground wood productivity. For this country-wide analysis, we used lidar data derived from a virtual lidar campaign over all BWI forest stands (for more details see methods 2.5). With this lidar data set, we created two maps for estimated horizontal and vertical structures of forests in Germany (Fig. 7). According to this analysis, 19% of all forest stands in Germany have a dense structure (horizontal structure with TCH > 18 m), which corresponds to high and closed forests. Only 10% of all forests have an open structure (horizontal structure with TCH < 6 m), which means that these stands are either low in height or have a low tree density. The mean value of TCH—the proxy for horizontal structure—for Germany is 12.4 m. The amount of forest area with heterogeneous vertical structure ($SD_{\text{VFP}} > 6$ m) is with 6% low compared to the amount of forest areas with simple vertical structure (20%, $SD_{\text{VFP}} < 2$ m). Most stands in Germany represent a medium value of heterogeneity in vertical structure (60%, SD_{VFP} between 2 m and 4 m) which corresponds to forests with a low number of layers. For whole Germany, the mean value of SD_{VFP}—the proxy for the vertical forest structure—is 3.1 m. Overall, according to this study, we have large areas with dense forests in Germany, but these forests are often less vertically structured with only one to two layers.

The densest forests can be found in the northern part and in the southern part of Germany. Within Germany, there is a trend for the horizontal structure to become increasingly dense from north to south (Fig. 16a). Looking at the east–west gradient of the
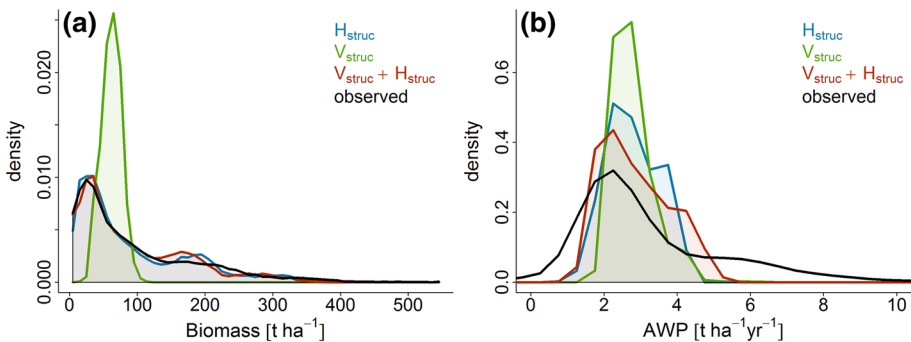
Fig. 6 Histogram for estimated forest biomass (**a**) and aboveground woody productivity (AWP, **b**) for all forest stands from the forest factory data set. Each of this forest attributes was estimated with the three approaches: H_{struc}—horizontal structure, V_{struc}—vertical structure and $H_{\text{struc}} + V_{\text{struc}}$—horizontal and vertical structures. The histograms of the estimated values were compared with the observed values from all forest stands (black line). The detailed relationships between estimated and observed biomass/productivity are presented in Figs. 9 and 10

**(a)** horizontal structure

(b) vertical structure
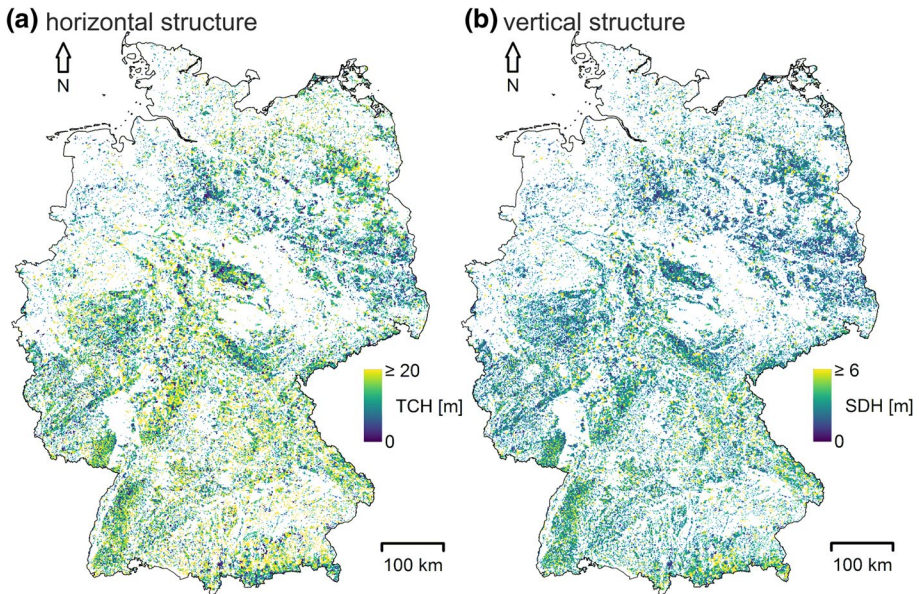
Fig. 7 Horizontal and vertical forest structures for Germany estimated from 3D remote sensing. As horizontal index for forest structure, we used top-of-canopy height (as proxy for the density of a forest stand), and as index for the vertical heterogeneity, the standard deviation of the vertical foliage profile was used. Low values of vertical structure stand for a homogenous structure, higher values for a heterogeneous structure

horizontal structure, however, one finds the densest stands in the middle region; at the outer edges, the horizontal structure is rather open (Fig. 16c). A similar pattern emerges for the vertical structural index with the most heterogeneous stands in the southern part of Germany (Fig. 16b). Regarding the relationship between horizontal forest structure and topographic gradients, no clear trend was observable (Fig. 16e). What can be detected, however, is that the variability of open and dense forests stands increases significantly for altitudes higher than 1000 m (Fig. 16e). The same applies to the vertical structure (Fig. 16f). In addition, a clear trend can be identified with vertically homogeneous stands at lower altitudes and vertically heterogeneous stands at higher altitudes (Fig. 16f).

Three regions in Germany show a high structural heterogeneity: the Black Forest, the Bavarian Forest and the mid-Alpine foothills. Looking at the described structural characteristics especially for forest areas in national parks and for forest areas outside national parks, there are only minor differences (Fig. 17). The horizontal structure of these forest stands is similar (TCH national park: 11.7 m vs. TCH non-national park: 12.4 m) and the vertical structure as well (SD_{VFP} national park: 3.3 m vs. SD_{VFP} non-national park: 3.1 m).

Using the estimated horizontal and vertical forest structures of each stand in Germany (cf., Fig. 7), it is possible now to estimate forest biomass and aboveground wood productivity. Applying the best approach $H_{struct} + V_{struct}$ (as shown in Table 1), we produced a forest biomass and aboveground wood productivity map for Germany (Fig. 8). In southern Germany we found higher biomass values compared to the north. The total
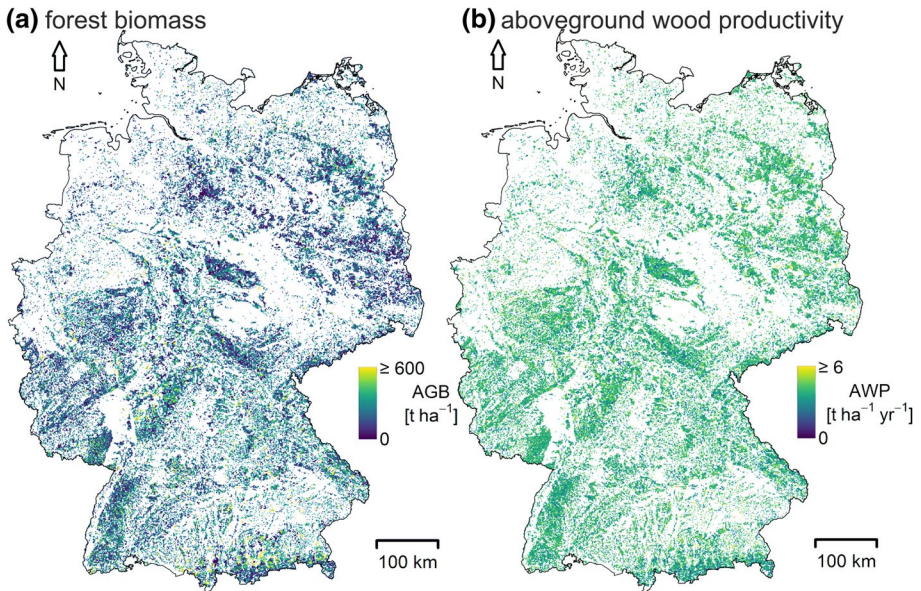
Fig. 8 Estimation of **a** forest biomass and **b** aboveground wood productivity for Germany by applying the $H_{struct} + V_{struct}$ approach. The $H_{struct} + V_{struct}$ approach was calibrated using all forest stands from the forest factory data set (cf., Table 1). Structural information for each forest stand was taken from Fig. 7

biomass of all forested areas in Germany is 2.3 Gt, and the mean biomass of forested areas is 209 t/ha. We estimated a total aboveground wood productivity of 43 Mt/year with a mean value of 4 t/ha/year.

We obtained a good agreement when comparing the estimated biomass ($H_{struct} + V_{struct}$ approach) with the observed biomass from the BWI plots ($r^2 = 0.76$, RMSE $= 65$ t/ha; cf. Fig. 14). Using only horizontal structural information produces also good results for the biomass estimation ($r^2 = 0.76$, RMSE $= 66$ t/ha, cf. Fig. 14). However, if only vertical structure is used as input, the results are poor ($r^2 = 0.14$, RMSE $= 125$ t/ha, cf. Fig. 14). This shows that for the estimation of the biomass, the information about the horizontal structure is sufficient.

4 Discussion

Forest structure is usually quantified using tree sizes from inventory measurements. In this study, we estimated forest structure from remote sensing (lidar) and provide a workflow to generate forest structure maps for Germany.

4.1 Estimating Horizontal and Vertical Forest Structures

For each structural dimension, a metric was found which could be used to determine horizontal and vertical forest structures. It was harder to find a metric for the vertical structure. For the measurement of vertical forest structure by remote sensing, standard deviation of the vertical foliage profile is very well suited to reflect the heterogeneity in the vertical leaf

distribution. For the estimation of the horizontal structure, top-of-canopy height (TCH) was selected, which is a height measurement and at first glance not a structural measure. However, TCH is a quite general metric that covers also information on the forest structure. On the one hand, it is affected by the height and shape of the largest trees in the upper canopy and is therefore closely linked to the basal area of these canopy trees. On the other hand, TCH also provides information about the horizontal vegetation density and the openness of a forest stand, if, for example, canopy gaps occur (Lu et al. 2016). For these reasons, TCH is suited to describe the density of a forest and thus its horizontal structure. However, horizontal structure can be also described by other approaches, which more closely include the positions of all trees. For example, the concepts of point pattern analysis could be used for this purpose (Wiegand et al. 2013). This would require identifying all individual trees from remote sensing, which has so far only been tested for small areas (e.g., Ferraz et al. 2016).

4.2 The Role of Forest Structure for Biomass and Productivity

For the estimation of forest biomass and productivity, the concept of forest structure classification in combination with forest modeling and remote sensing has a high potential for applications on larger scales. For 375,000 forest stands, we have investigated the relations between structure, biomass and aboveground wood productivity in forest ecosystems. Forest structure has been shown to be an important factor for estimating biomass and productivity from remote sensing. In particular, horizontal forest structure seems to be a good predictor for forest biomass, while the vertical forest structure showed only weaker relationships with forest biomass. Hence, metrics describing the horizontal structure of forests might be a good choice for forest biomass estimations which is in accordance with other studies (Asner and Mascaro 2014; Knapp et al. 2018a). Metrics describing the vertical structural (e.g., the standard deviation of the vertical foliage profile) are useful for forest productivity estimations. Vertical foliage profile showed a much higher correlation with the ground-based standard deviation of tree heights than the standard deviation of the classical canopy height model profile. With VFP, the weight of larger and smaller canopy trees is the same, while classical lidar profiles are dominated by upper canopy trees. Small canopy trees may only provide a minor contribution to stand biomass, but can play an important role for stand productivity—which emphasizes the role of vertical structure for productivity estimations (Bohn and Huth 2017). In a study by Stark et al. (2012), the Shannon index of the lidar profile was successfully related to forest dynamics like productivity and mortality rates. In our study, this Shannon index performed also very well as vertical metric, as it measures the heterogeneity of leaf densities in different layers.

Our aim was to estimate forest structure from a single remote sensing measurement and use this information for improved biomass and productivity estimations. An alternative approach for productivity estimations would be to analyze the change in forest structure and relate this to biomass change or productivity. For example, with lidar or radar it is possible to detect larger changes in forest height over a certain time period. However, often an exact detection of the height change via remote sensing is not possible, because particularly old-growth forests rarely change their canopy height and the detection error of the sensor is often larger than the actual change in height (e.g., Knapp et al. 2018b). In addition, data are often only available for a single remote sensing campaign (e.g., country-wide airborne lidar campaigns). Therefore, there is a strong need for the estimation of forest productivity from forest structure.

We assume a simplified Central European climate and sites with homogenous soil conditions, without any spatial heterogeneities. This has the advantage of eliminating the influence of changing climate and soil properties on biomass and productivity estimations. It allowed to study the fundamental role of forest structure on biomass and productivity. Future studies will investigate the influence of changing environmental factors on these estimations.

In perspective, information about forest structure can be used to distinguish different forest types, for example natural forests, forests that are disturbed by natural hazards or forests that have been managed by different strategies (Dieler et al. 2017; Müller et al. 2000; Peck et al. 2014; Young et al. 2017). It is also worthwhile to consider forest structure in the context of biodiversity research (Jetz et al. 2016; Pereira et al. 2013; Pettorelli et al. 2016). Forest structure can be a valuable indicator of biodiversity, since habitat structure and habitat heterogeneity can be correlated with animal and plant species diversity (e.g., Boncina 2000; Ishii et al. 2004; Schall et al. 2018a; Tews et al. 2004). All of this emphasizes the need for large-scale forest structure estimations from remote sensing.

4.3 Linking Forest Models with Remote Sensing

In this study, the role of forest structure for biomass and productivity estimations was investigated by analyzing a large data set generated from a forest model. The synergy of forest models with remote sensing is a promising method. Structural realism in a model is a requirement for applying such a concept, which was realized here by the individual-based approach of the FORMIND model (Fischer et al. 2016; Shugart et al. 2015). In particular, forest gap models are helpful tools to understand forest responses to climate change, modified disturbance regimes and structural changes (Shugart et al. 2018). A few studies have tried to link remote sensing and forest modeling, covering model parameterization and initialization (Falkowski et al. 2010; Hurtt et al. 2004; Ranson et al. 2001), exploring several remote sensing metrics for ecosystem service estimations (Knapp et al. 2018a; Köhler and Huth 2010; Palace et al. 2015) and for error quantification (Frazer et al. 2011; Hurtt et al. 2010).

To sum up, forest models can help to find reliable estimates of forest biomass and productivity as presented in this study. Gap models are particularly valuable because they take into account not only large-scale disturbances but also small-scale variations of forest structures (due to gap-building processes). Linking forest models with remote sensing can help to extrapolate local findings to larger scales and better understand ecosystem patterns and processes (Knapp et al. 2018b; Rödig et al. 2017, 2018).

Here, we used information from airborne lidar remote sensing—however, this analysis is not limited to airborne lidar, but can also be applied to other remote sensing techniques such as lidar and radar satellite missions. Therefore, the forest structure classification presented here can be applied also to other regions. Measurements of the upcoming satellite missions will offer a unique opportunity to reduce the uncertainties in the estimation of aboveground carbon emissions from forests (resulting from photosynthesis, respiration, mortality, human disturbances). These missions will also provide the opportunity to identify changes in forest structure which can be relevant for the estimation of forest productivity. This will improve our understanding of the global carbon cycle, which will be relevant for climate modeling and policy adaptation.

5 Conclusion

In this study, we applied a novel approach of linking remote sensing measurements with dynamic forest models to study the role of forest structure for biomass and productivity. While information on horizontal structure seems to be sufficient for estimating biomass, information on horizontal and vertical structures is required for estimating aboveground wood productivity. In a case study for Germany, maps for forest structure, biomass and aboveground wood productivity were provided. The presented workflow is transferable to other regions as remote sensing data are available. Future satellite missions that measure forest structure (like GEDI from 2018, BIOMASS from 2020 and Tandem-L expected from 2022) will allow the derivation of more accurate estimations of forest biomass, productivity and other forest ecosystem services.

Appendix 1: Estimation of Forest Attributes Using Structural Information

Describing Forest Structure from Field Data

The study examined a total of 13 field-based metrics to describe forest structure, which are listed in the following. Forest structure was described, for example, by basal area BA [m^2], which is the sum of all tree basal area values BA_i of a forest stand:

$$BA = \sum_i BA_i = \sum_i \frac{\pi}{4} d_i^2,$$

where d_i (m) is the stem diameter of a tree i (in total n trees in a stand). Alternative metrics to describe the horizontal and vertical structures of a forest stand are:

standard deviation of stem diameters: $SD_{DBH} = \sqrt{\frac{1}{n-1} \sum_i \left(d_i - \bar{d}\right)^2}$

coefficient of variation of all stem diameters: $CV_{DBH} = \frac{SD_{DBH}}{\bar{d_i}}$

skewness of the diameter distribution: $Skew_{DBH} = \frac{\frac{1}{n} \cdot \sum_{i=1}^{n} \left(d_i - \bar{d}\right)^3}{\left(\frac{1}{n} \cdot \sum_{i=1}^{n} \left(d_i - \bar{d}\right)^2\right)^{\frac{3}{2}}}$

Gini coefficient of the diameter distribution: $Gini_{DBH} = \frac{2 \sum_i i \cdot d_i}{n \sum_i d_i} - \frac{n+1}{n}$, where d_i is the sorted list of stem diameters.

$\bar{d}$ is the mean diameter of all trees within a stand. The same metrics can be calculated also for the tree height distribution (where H_i (m) is the height of a tree) or basal area distribution. Especially for the tree height distribution, we have calculated further metrics.

maximum height: $H_{\max} = \max\left(H_i\right)$

mean height: $H_{\text{mean}} = \frac{1}{n}\sum_i H_i$

quadratic mean height: $H_{\text{quad·mean}} = \sqrt{\frac{1}{n}\sum_i H_i^{2i}}$

Lorey's height: $H_{\text{Lorey's}} = \frac{\sum_i H_i \cdot \text{BA}_i}{\sum_i \text{BA}_i}$.

Describing Forest Structure from Remote Sensing Data

Estimating forest structure from remote sensing is more challenging as remote sensing data are not tree-based as in the field-based case. This study examined a total of 25 remote sensing-based metrics to describe forest structure. The basis for most metrics is the lidar-derived canopy height model (CHM) with a spatial resolution of 1 m×1 m. In this study, we described horizontal structure for each 20 m×20 m forest stand mainly by the mean top-of-canopy height TCH (m), which is the mean of the canopy height model (CHM):

$$\text{TCH} = \frac{\sum_{i=1}^{n} P_{\text{CHM},i}}{n},$$

where $P_{\text{CHM},i}$ is the forest height of the CHM in pixel i and n is the number of pixels. Alternative metrics based on the CHM are:

maximum height: $H_{\max} = \max\left(P_{\text{CHM},i}\right)$

quadratic TCH: $\text{QTCH} = \sqrt{\frac{\sum_{i=1}^{n} P_{\text{CHM},i}^2}{n}}$

relative height of the CHM: $\text{RH}_q = \text{quantile}_q\left(P_{\text{CHM},i}\right)$

It is also possible to calculate the standard deviation, the coefficient of variation and the skewness of the CHM (functions are described above in the field-based section). In this study, we considered further advanced metrics based on the CHM:

Shannon index of the CHM: $\text{Shannon}_{\text{CHM}} = -\sum_{i=1}^{i\max} \text{CHM}\left(h_i\right) \cdot \ln\left(\text{CHM}\left(h_i\right)\right),$

with CHM (h_i) being the CHM profile value (pixel count) in bin i. CHM (h_i) has to be >0, and CHM $(h_i)=0$ is ignored,

Kurtosis of the CHM: $\text{Kurtosis}_{\text{CHM}} = n \cdot \dfrac{\sum_{i=1}^{n}\left(P_{\text{CHM},i}-\overline{P_{\text{CHM}}}\right)^4}{\left(\sum_{i=1}^{n}\left(P_{\text{CHM},i}-\overline{P_{\text{CHM}}}\right)^2\right)^2},$

with n being the total pixel number, $P_{\text{CHM},i}$ the value of pixel i and $\overline{P_{\text{CHM}}}$ the mean value of the CHM (which is the same as TCH),

the p–h ratio of the CHM: $P:H_{\text{CHM}} = \dfrac{h\left(\max\limits_{i\in[1,i_{\max}]}\left(\text{CHM}(h_i)\right)\right)}{\max\limits_{i\in[1,i_{\max}]}\left(h_i\right)},$

with CHM (h_i) being the pixel count in height bin h_i and i_{max} is the highest height bin.

Another class of metrics calculates the fractional canopy cover above a certain threshold $\times$ (m) using the CHM: $\text{FCC}_x = \frac{\sum_{h_i=x}^{h}\text{max CHM}(h_i)}{\sum_{h_i=0}^{h}\text{max CHM}(h_i)}$, with CHM (h_i) the count of CHM pixels in height bin h_i and $\times$ the height threshold to distinguish canopy from gap.

Instead of using the CHM as the basic information for calculating all these lidar metrics, we have used the vertical foliage profile (VFP) for a second class of metrics. All the above-described metrics can be calculated using the VFP. For this reason, the VFP was divided into 1-m height classes. This height classes can now be used in the equations described above by replacing the CHM. The generation of a VFP profile from a CHM is described below.

## Calculating the Vertical Foliage Profile from a CHM

The vertical foliage profile (VFP) was reconstructed from the CHM profile at 1 m vertical resolution following the approach described by Harding et al. (2001).

$$\text{VFP}(h_i) = \frac{1}{k * \Delta h} * \ln\left(\frac{P(h_i)}{P(h_{i+1})}\right),$$

with k being the light extinction coefficient, Δh the width of one height bin and $P(h_i)$ the value of the cumulative CHM profile in height bin h_i. The method reconstructs the vertical leaf profile by giving more weight to lower parts of the profile. All pixels below 5 m height were regarded as ground and the light extinction coefficient was set to 0.3 which has been shown to result in good LAI estimations (Getzin et al. 2017).

Estimation of Forest Biomass and Productivity Using Forest Structure

See Figs. 9 and 10.
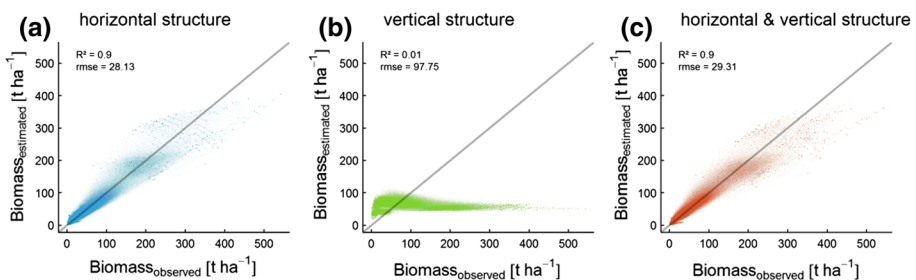
Fig. 9 Relationship between observed biomass and estimated biomass derived by three different approaches (see Table 1). Each point represents one of 375,000 forest stands from the forest factory data set. The observed biomass have been derived by summing up the biomass values of all trees in the 20 m $\times$ 20 m stand. The estimated biomass was determined using the structural information for each forest stand. **a** Estimation of biomass using only information from the horizontal structural index TCH (AGB $= 9.49 * \text{TCH}^{1.22}$, $r^2 = 0.90$), **b** using the vertical structural index SD_{VFP} (AGB $= 34.77 * \text{SD}_{\text{VFP}}^{0.48}$, $r^2 = 0.01$) and **c** using the vertical and horizontal structural index (AGB $= 7.55 * \text{TCH}^{1.20} * \text{SD}_{\text{VFP}}^{0.23}$, $r^2 = 0.90$). A comparison of the estimated biomass values for the different approaches is shown in Fig. 6a
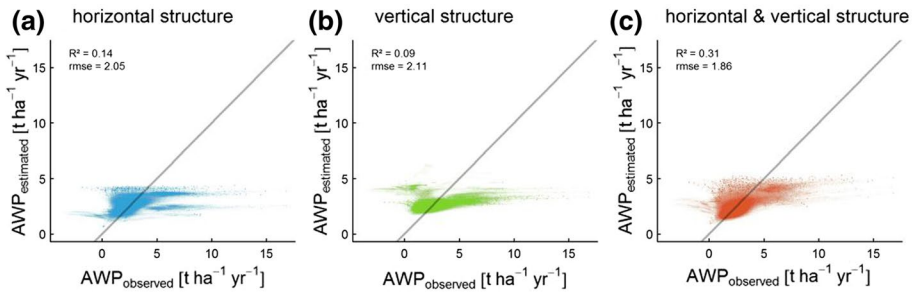
Fig. 10 Relationship between observed and estimated aboveground woody productivity (AWP) for 375,000 forest stands (forest factory data set). Each dot represents one forest stand. **a** Estimation of productivity using only the horizontal structural index TCH (AWP $= 1.68 * \text{TCH}^{0.31}$, $r^2 = 0.14$), **b** only the vertical structural index SD_{VFP} (AWP $= 4.03 * \text{SD}_{\text{VFP}}^{-0.34}$, $r^2 = 0.09$) and **c** using the vertical and horizontal structural index (AWP $= 2.55 * \text{TCH}^{0.34} * \text{SD}_{\text{VFP}}^{-0.39}$, $r^2 = 0.31$). A comparison of the estimated productivity values with the different approaches is shown in Fig. 6b

Appendix 2: Analysis of the German Forest Inventory Data Set

All analyses so far referred to the forest factory data set. This Appendix reproduces all analyses with the empirical BWI data set. For each forest stand of the BWI data set, a virtual lidar campaign was carried out and the remote sensing-based metrics were then calculated.

See Figs. 11, 12, 13, 14, 15, 16 and 17.
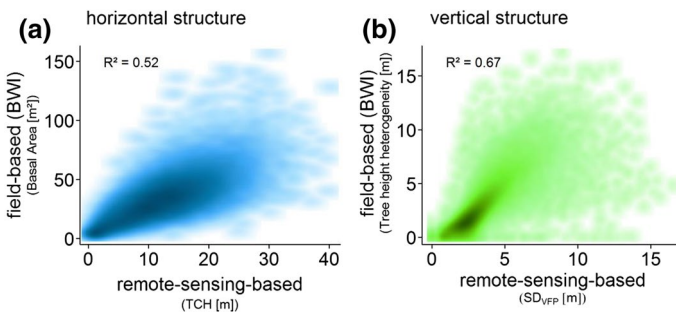
Fig. 11 Remote sensing-based estimation of the forest structure using the BWI data set. Each dot represents one stand of the BWI. The figure shows the estimate of **a** the horizontal forest structure (basal area) from lidar using top-of-canopy height and **b** the vertical forest structure (tree height heterogeneity) from lidar using the standard deviation of the vertical foliage profile

	Max. H	TCH	QTCH	RH75 (CHM)	RH50 (CHM)	FCC0	FCC10	FCC20	MCH (VFP)	QMCH (VFP)	RH75 (VFP)	RH50 (VFP)	SD (CHM)	CV (CHM)	Shannon Index (CHM)	P·H ratio (CHM)	Skewness (CHM)	Kurtosis (CHM)	SD (VFP)	CV (VFP)	Shannon Index (VFP)	Gini Index (VFP)	P·H ratio (VFP)	Skewness (VFP)	Kurtosis (VFP)	Observed AGB
Observed AGB	0.36	0.76	0.66	0.51	0.63	0.60	0.59	0.57	0.33	0.33	0.33	0.33	0.22	0.43	0.36	0.11	0.59	0.00	0.12	0.00	0.18	0.02	0.00	0.06	0.02	1.00
BA	0.14	0.52	0.39	0.30	0.49	0.69	0.60	0.29	0.10	0.10	0.11	0.10	0.06	0.51	0.55	0.13	0.64	0.00	0.07	0.01	0.27	0.13	0.00	0.02	0.01	0.74
Max. tree H	0.97	0.64	0.82	0.72	0.37	0.18	0.33	0.67	0.92	0.94	0.96	0.94	0.87	0.15	0.07	0.08	0.17	0.00	0.33	0.00	0.17	0.03	0.00	0.09	0.03	0.38
Mean tree H	0.69	0.45	0.60	0.52	0.26	0.07	0.20	0.52	0.86	0.84	0.72	0.76	0.70	0.07	0.00	0.01	0.10	0.00	0.01	0.19	0.01	0.20	0.07	0.07	0.02	0.24
Quad. mean tree H	0.74	0.48	0.64	0.56	0.28	0.08	0.22	0.55	0.90	0.88	0.77	0.80	0.74	0.07	0.00	0.00	0.11	0.00	0.02	0.16	0.02	0.19	0.07	0.09	0.02	0.26
Lorey's H	0.90	0.60	0.78	0.68	0.35	0.12	0.28	0.66	0.99	0.99	0.94	0.95	0.87	0.11	0.02	0.03	0.15	0.00	0.15	0.04	0.07	0.11	0.04	0.14	0.04	0.34
Mean tree H / Max. tree H	0.02	0.01	0.01	0.01	0.01	0.03	0.00	0.01	0.00	0.01	0.00	0.00	0.00	0.05	0.18	0.40	0.02	0.01	0.57	0.74	0.33	0.35	0.23	0.00	0.01	0.02
Lorey's H / Max. tree H	0.00	0.00	0.00	0.00	0.00	0.06	0.02	0.01	0.04	0.03	0.00	0.01	0.00	0.06	0.22	0.15	0.02	0.02	0.34	0.35	0.42	0.42	0.09	0.00	0.00	0.00
CV (BA)	0.04	0.04	0.04	0.04	0.03	0.10	0.06	0.02	0.00	0.00	0.00	0.00	0.00	0.08	0.17	0.31	0.05	0.01	0.47	0.51	0.26	0.22	0.13	0.00	0.00	0.05
CV (DBH)	0.05	0.08	0.07	0.07	0.06	0.15	0.10	0.04	0.00	0.01	0.04	0.02	0.02	0.12	0.23	0.43	0.09	0.01	0.48	0.44	0.33	0.27	0.08	0.02	0.01	0.09
Skewness (DBH)	0.00	0.00	0.00	0.00	0.00	0.01	0.00	0.01	0.03	0.02	0.00	0.01	0.01	0.01	0.04	0.01	0.00	0.00	0.12	0.27	0.07	0.09	0.21	0.09	0.00	0.00
SD tree H	0.18	0.17	0.17	0.17	0.10	0.13	0.12	0.13	0.07	0.09	0.16	0.14	0.12	0.10	0.17	0.61	0.08	0.00	0.67	0.37	0.33	0.17	0.02	0.15	0.07	0.13
CV tree H	0.03	0.02	0.02	0.03	0.01	0.05	0.03	0.01	0.00	0.00	0.02	0.01	0.01	0.04	0.12	0.57	0.02	0.00	0.57	0.58	0.24	0.22	0.07	0.09	0.04	0.03
Skewness tree H	0.00	0.02	0.02	0.01	0.03	0.01	0.02	0.02	0.01	0.01	0.00	0.01	0.00	0.00	0.02	0.00	0.00	0.00	0.10	0.23	0.01	0.01	0.20	0.15	0.01	0.02

Fig. 12 Overview of all correlations between field-based structural metrics and remote sensing-based metrics based only on the BWI data set. Numbers and gray scale indicate the coefficient of determination. All structural metrics are explained in Appendix 1
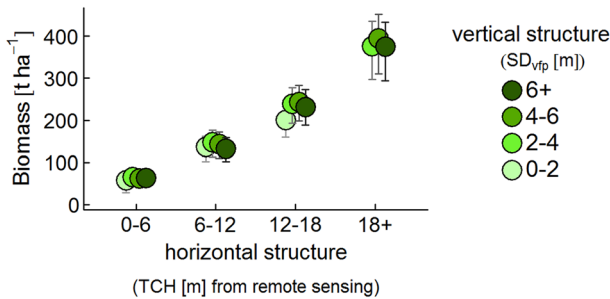

Fig. 13 Role of forest structure for biomass, derived from the BWI data set (more than 45,000 field plots, 20 m × 20 m). Forest structure is estimated from remote sensing. As horizontal forest structure descriptor the top-of-canopy height (TCH) was used and as vertical structure descriptor the standard deviation of the vertical foliage profile (SD$_{VFP}$). Shown is the mean aboveground biomass in relation to the forest structure classes. Error bars indicate the standard deviation
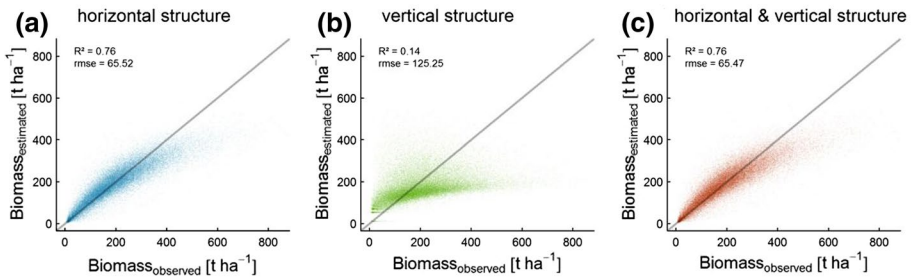
Fig. 14 Relationship between observed biomass and estimated biomass. Each point represents one forest stand from the forest inventory data set BWI. The observed biomass has been taken from the BWI data set. The estimated biomass values were determined using different approaches (cf. Table 1) and information on forest structure. **a** Estimation of biomass using only the horizontal structural index TCH, **b** only the vertical structural index SD_{VFP} and **c** using the vertical and horizontal structural index. A comparison of the estimated values with the different approaches is shown in Fig. 15

Fig. 15 Histogram for forest biomass estimates for Germany based on the BWI data set. The biomass was estimated using three different approaches: *H*—horizontal structure (blue), *V*—vertical structure (green) and *H* + *V*—horizontal and vertical structures (red). The histogram was compared with the measured values from the BWI data set (black line)

(a) horizontal structure **(b)** vertical structure
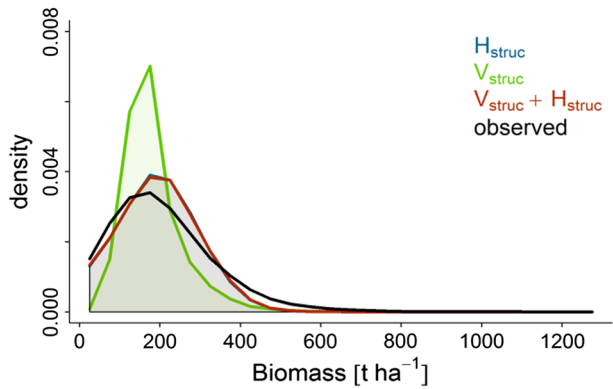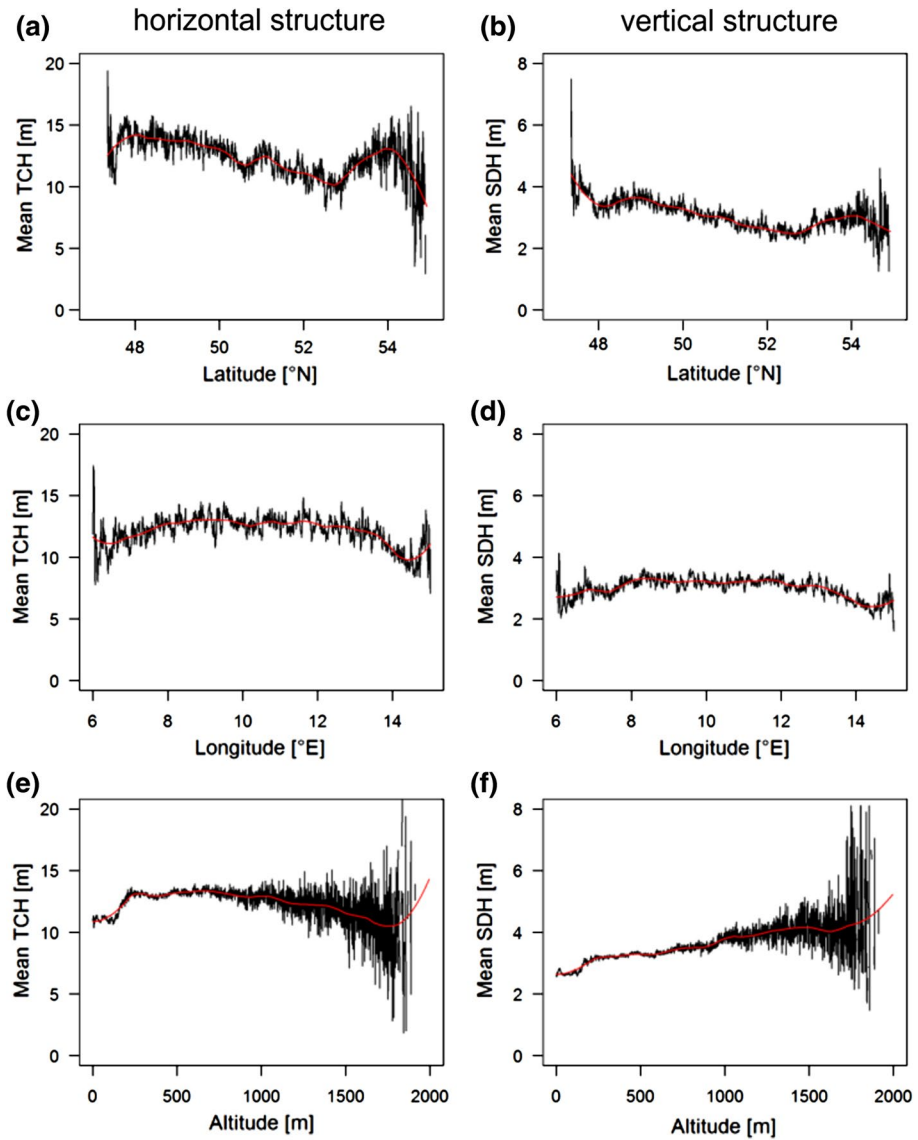
Fig. 16 Forest structure of Germany over different gradients. Mean value of the horizontal structure (TCH) from **a** south to north, **c** west to east in Germany and **e** over the altitudinal gradient. Mean value of the vertical structure (SD$_{VFP}$) from **a** south to north, **c** west to east in Germany and **e** over the altitudinal gradient. The structure values correspond to Fig. 7 (forest structure maps of Germany)
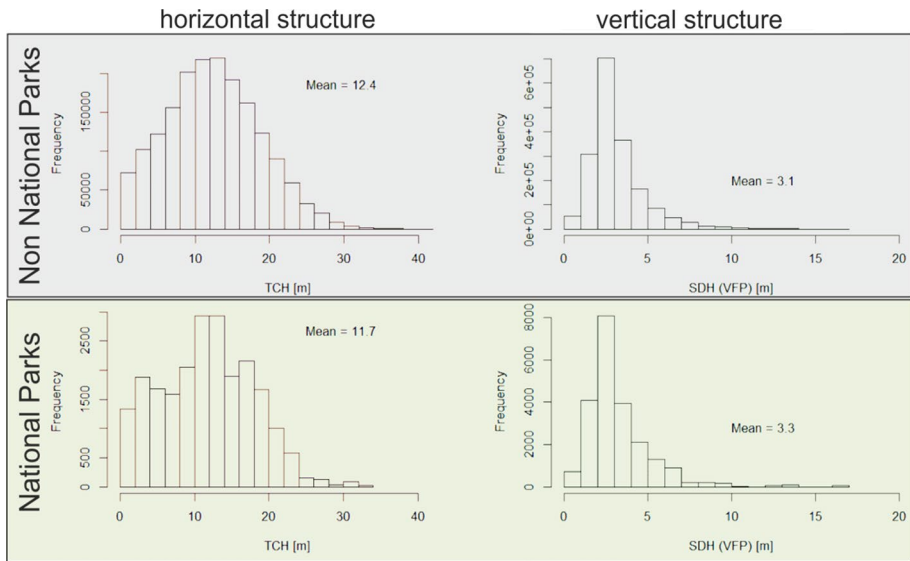
Fig. 17 Histograms of structural metrics for forests outside of national parks and inside national parks. As horizontal forest structure descriptor, the top-of-canopy height (TCH, left) was used, and as vertical structure descriptor, the standard deviation of the vertical foliage profile (SD$_{VFP}$, right) was used

References

Asner GP, Mascaro J (2014) Mapping tropical forest carbon: calibrating plot estimates to a simple LiDAR metric. Remote Sens Environ 140:614–624

Bohn FJ, Huth A (2017) The importance of forest structure to biodiversity–productivity relationships. R Soc Open Sci 4:160521

Bohn FJ, Frank K, Huth A (2014) Of climate and its resulting tree growth: simulating the productivity of temperate forests. Ecol Model 278:9–17

Bonan GB (2008) Forests and climate change: forcings, feedbacks, and the climate benefits of forests. Science 320:1444–1449

Boncina A (2000) Comparison of structure and biodiversity in the Rajhenav virgin forest remnant and managed forest in the Dinaric region of Slovenia. Glob Ecol Biogeogr 9:201–211

Cazcarra-Bes V, Tello-Alonso M, Fischer R, Heym M, Papathanassiou K (2017) Monitoring of forest structure dynamics by means of L-band SAR tomography. Remote Sens 9:1229

Dănescu A, Albrecht AT, Bauhus J (2016) Structural diversity promotes productivity of mixed, uneven-aged forests in southwestern Germany. Oecologia 182:319–333

del Río M, Pretzsch H, Alberdi I, Bielak K, Bravo F, Brunner A, Condés S, Ducey MJ, Fonseca T, von Lüpke N, Pach M, Peric S, Perot T, Souidi Z, Spathelf P, Sterba H, Tijardovic M, Tomé M, Vallet P, Bravo-Oviedo A (2016) Characterization of the structure, dynamics, and productivity of mixed-species stands: review and perspectives. Eur J For Res 135:23–49

Dieler J, Uhl E, Biber P, Müller J, Rötzer T, Pretzsch H (2017) Effect of forest stand management on species composition, structural diversity, and productivity in the temperate zone of Europe. Eur J For Res 136:739–766

Disney M (2018) Terrestrial Li DAR: a three-dimensional revolution in how we look at trees. New Phytol. https://doi.org/10.1111/nph.15517

Dobbertin M (2002) Influence of stand structure and site factors on wind damage—comparing the storms Vivian and Lothar. For Snow Landsc Res 77:187–205

Dubayah RO, Sheldon SL, Clark DB, Hofton MA, Blair JB, Hurtt GC, Chazdon RL (2010) Estimation of tropical forest height and biomass dynamics using lidar remote sensing at La Selva, Costa Rica. J Geophys Res Biogeosci 115:G00E09

Exbrayat J-F, Bloom AA, Carvalhais N, Fischer R, Huth A, MacBean N, Williams M (2019) Understanding the land carbon cycle with space data: current status and prospects. Surv Geophys. https://doi.org/10.1007/s10712-019-09506-2

Falkowski MJ, Hudak AT, Crookston NL, Gessler PE, Uebler EH, Smith AMS (2010) Landscape-scale parameterization of a tree-level forest growth model: a k-nearest neighbor imputation approach incorporating LiDAR data. Can J For Res 40:184–199

Ferraz A, Saatchi S, Mallet C, Meyer V (2016) Lidar detection of individual tree size in tropical forests. Remote Sens Environ 183:318–333

Fischer R, Bohn F, Dantas de Paula M, Dislich C, Groeneveld J, Gutiérrez AG, Kazmierczak M, Knapp N, Lehmann S, Paulick S, Pütz S, Rödig E, Taubert F, Köhler P, Huth A (2016) Lessons learned from applying a forest gap model to understand ecosystem and carbon dynamics of complex tropical forests. Ecol Model 326:124–133

Fischer R, Knapp N, Bohn F, Huth A (2019) Remote sensing measurements of forest structure types for ecosystem service mapping. In: Schröter M, Bonn A, Klotz S, Seppelt R, Baessler C (eds) Atlas of ecosystem services: drivers, risks, and societal responses. Springer, Cham, pp 63–67

Foley JA, DeFries R, Asner GP, Barford C, Bonan G, Carpenter SR, Chapin FS, Coe MT, Daily GC, Gibbs HK, Helkowski JH, Holloway T, Howard EA, Kucharik CJ, Monfreda C, Patz JA, Prentice IC, Ramankutty N, Snyder PK (2005) Global consequences of land use. Science 309:570–574

Frazer GW, Magnussen S, Wulder MA, Niemann KO (2011) Simulated impact of sample plot size and co-registration error on the accuracy and uncertainty of LiDAR-derived estimates of forest stand biomass. Remote Sens Environ 115:636–649

Getzin S, Fischer R, Knapp N, Huth A (2017) Using airborne LiDAR to assess spatial heterogeneity in forest structure on Mount Kilimanjaro. Landsc Ecol 32:1881–1894

Grace J, Mitchard E, Gloor E (2014) Perturbations in the carbon budget of the tropics. Glob Change Biol 20:3238–3255

Hansen MC, Potapov PV, Moore R, Hancher M, Turubanova SA, Tyukavina A, Thau D, Stehman SV, Goetz SJ, Loveland TR, Kommareddy A, Egorov A, Chini L, Justice CO, Townshend JRG (2013) High-resolution global maps of 21st-century forest cover change. Science 342:850–853

Hardiman BS, Bohrer G, Gough CM, Vogel CS, Curtis PS (2011) The role of canopy structural complexity in wood net primary production of a maturing northern deciduous forest. Ecology 92:1818–1827

Harding DJ, Lefsky MA, Parker GG, Blair JB (2001) Laser altimeter canopy height profiles: methods and validation for closed-canopy, broadleaf forests. Remote Sens Environ 76:283–297

Houghton RA, Lawrence KT, Hackler JL, Brown S (2001) The spatial distribution of forest biomass in the Brazilian Amazon: a comparison of estimates. Glob Change Biol 7:731–746

Hurtt GC, Dubayah R, Drake J, Moorcroft PR, Pacala SW, Blair JB, Fearon MG (2004) Beyond potential vegetation: combining lidar data and a height-structured model for carbon studies. Ecol Appl 14:873–883

Hurtt GC, Fisk J, Thomas RQ, Dubayah R, Moorcroft PR, Shugart HH (2010) Linking models and data on vegetation structure. J Geophys Res Biogeosci. https://doi.org/10.1029/2009JG000937

Ishii HT, Tanabe S, Hiura T (2004) Exploring the relationships among canopy structure, stand productivity, and biodiversity of temperate forest ecosystems. For Sci 50:342–355

Jetz W, Cavender-Bares J, Pavlick R, Schimel D, Davis FW, Asner GP, Guralnick R, Kattge J, Latimer AM, Moorcroft P, Schaepman ME, Schildhauer MP, Schneider FD, Schrodt F, Stahl U, Ustin SL (2016) Monitoring plant functional diversity from space. Nat Plants 2:16024

Knapp N, Fischer R, Huth A (2018a) Linking lidar and forest modeling to assess biomass estimation across scales and disturbance states. Remote Sens Environ 205:199–209

Knapp N, Huth A, Kugler F, Papathanassiou K, Condit R, Hubbell SP, Fischer R (2018b) Model-assisted estimation of tropical forest biomass change: a comparison of approaches. Remote Sens 10:731

Köhler P, Huth A (2010) Towards ground-truthing of spaceborne estimates of above-ground life biomass and leaf area index in tropical rain forests. Biogeosciences 7:2531–2543

Lefsky MA (2010) A global forest canopy height map from the moderate resolution imaging spectroradiometer and the geoscience laser altimeter system. Geophys Res Lett 37:L15401

Lefsky MA, Harding D, Cohen WB, Parker G, Shugart HH (1999) Surface lidar remote sensing of basal area and biomass in deciduous forests of eastern Maryland, USA. Remote Sens Environ 67:83–98

Liang JJ, Crowther TW, Picard N, Wiser S, Zhou M, Alberti G, Schulze ED, McGuire AD, Bozzato F, Pretzsch H, de-Miguel S, Paquette A, Hérault B, Scherer-Lorenzen M, Barrett CB, Glick HB, Hengeveld GM, Nabuurs GJ, Pfautsch S, Viana H, Vibrans AC, Ammer C, Schall P, Verbyla D, Tchebakova N, Fischer M, Watson JV, Chen HYH, Lei XD, Schelhaas MJ, Lu HC, Gianelle D, Parfenova EI, Salas C, Lee E, Lee B, Kim HS, Bruelheide H, Coomes DA, Piotto D, Sunderland T, Schmid B, Gourlet-Fleury S, Sonké B, Tavani R, Zhu J, Brandl S, Vayreda J, Kitahara F, Searle EB, Neldner VJ, Ngugi MR, Baraloto C, Frizzera L, Balazy R, Oleksyn J, Zawiła-Niedźwiecki T, Bouriaud O, Bussotti F, Finér L, Jaroszewicz

B, Jucker T, Valladares F, Jagodzinski AM, Peri PL, Gonmadje C, Marthy W, O'Brien T, Martin EH, Marshall AR, Rovero F, Bitariho R, Niklaus PA, Alvarez-Loayza P, Chamuya N, Valencia R, Mortier F, Wortel V, Engone-Obiang NL, Ferreira LV, Odeke DE, Vasquez RM, Lewis SL, Reich PB (2016) Positive biodiversity–productivity relationship predominant in global forests. Science 354:196

Lu D, Chen Q, Wang G, Liu L, Li G, Moran E (2016) A survey of remote sensing-based aboveground biomass estimation methods in forest ecosystems. Int J Digit Earth 9:63–105

Malhi Y, Wood D, Baker TR, Wright J, Phillips OL, Cochrane T, Meir P, Chave J, Almeida S, Arroyo L, Higuchi N, Killeen TJ, Laurance SG, Laurance WF, Lewis SL, Monteagudo A, Neill DA, Vargas PN, Pitman NCA, Quesada CA, Salomão R, Silva JNM, Lezama AT, Terborgh J, Martinez RV, Vinceti B (2006) The regional variation of aboveground live biomass in old-growth Amazonian forests. Glob Change Biol 12:1107–1138

Müller S, Ammer C, Nüsslein S (2000) Analyses of stand structure as a tool for silvicultural decisions—a case study in a *Quercus petraea—Sorbus torminalis* stand. Forstwiss Cent 119:32–42

Palace MW, Sullivan FB, Ducey MJ, Treuhaft RN, Herrick C, Shimbo JZ, Mota-E-Silva J (2015) Estimating forest structure in a tropical forest using field measurements, a synthetic model and discrete return lidar data. Remote Sens Environ 161:1–11

Pan YD, Birdsey RA, Fang JY, Houghton R, Kauppi PE, Kurz WA, Phillips OL, Shvidenko A, Lewis SL, Canadell JG, Ciais P, Jackson RB, Pacala SW, McGuire AD, Piao SL, Rautiainen A, Sitch S, Hayes D (2011) A large and persistent carbon sink in the world's forests. Science 333:988–993

Peck JE, Zenner EK, Brang P, Zingg A (2014) Tree size distribution and abundance explain structural complexity differentially within stands of even-aged and uneven-aged structure types. Eur J For Res 133:335–346

Pereira HM, Ferrier S, Walters M, Geller GN, Jongman RHG, Scholes RJ, Bruford MW, Brummitt N, Butchart SHM, Cardoso AC, Coops NC, Dulloo E, Faith DP, Freyhof J, Gregory RD, Heip C, Hoft R, Hurtt G, Jetz W, Karp DS, McGeoch MA, Obura D, Onoda Y, Pettorelli N, Reyers B, Sayre R, Scharlemann JPW, Stuart SN, Turak E, Walpole M, Wegmann M (2013) Essential biodiversity variables. Science 339:277–278

Pettorelli N, Wegmann M, Skidmore A, Mücher S, Dawson TP, Fernandez M, Lucas R, Schaepman ME, Wang T, O'Connor B, Jongman RHG, Kempeneers P, Sonnenschein R, Leidner AK, Böhm M, He KS, Nagendra H, Dubois G, Fatoyinbo T, Hansen MC, Paganini M, de Klerk HM, Asner GP, Kerr JT, Estes AB, Schmeller DS, Heiden U, Rocchini D, Pereira HM, Turak E, Fernandez N, Lausch A, Cho MA, Alcaraz-Segura D, McGeoch MA, Turner W, Mueller A, St-Louis V, Penner J, Vihervaara P, Belward A, Reyers B, Geller GN (2016) Framing the concept of satellite remote sensing essential biodiversity variables: challenges and future directions. Remote Sens Ecol Conserv 2:122–131

Pommerening A (2002) Approaches to quantifying forest structures. Forestry 75:305–324

Pretzsch H (2009) Forest dynamics, growth and yield. Springer, Berlin

Pretzsch H, del Río M, Schütze G, Ammer C, Annighöfer P, Avdagic A, Barbeito I, Bielak K, Brazaitis G, Coll L, Drössler L, Fabrika M, Forrester DI, Kurylyak V, Löf M, Lombardi F, Matović B, Mohren F, Motta R, den Ouden J, Pach M, Ponette Q, Skrzyszewski J, Sramek V, Sterba H, Svoboda M, Verheyen K, Zlatanov T, Bravo-Oviedo A (2016) Mixing of Scots pine (*Pinus sylvestris* L.) and European beech (*Fagus sylvatica* L.) enhances structural heterogeneity, and the effect increases with water availability. For Ecol Manag 373:149–166

Ranson KJ, Sun G, Knox RG, Levine ER, Weishampel JF, Fifer ST (2001) Northern forest ecosystem dynamics using coupled models and remote sensing. Remote Sens Environ 75:291–302

Reineke LH (1933) Perfecting a stand-density index for even-aged forests. J Agric Res 46:627–638

Rödig E, Cuntz M, Heinke J, Rammig A, Huth A (2017) Spatial heterogeneity of biomass and forest structure of the Amazon rain forest: linking remote sensing, forest modelling and field inventory. Glob Ecol Biogeogr 26:1292–1302

Rödig E, Cuntz M, Rammig A, Fischer R, Taubert F, Huth A (2018) The importance of forest structure for carbon fluxes of the Amazon rainforest. Environ Res Lett 13:054013

Saatchi SS, Houghton RA, Alvala RCDS, Soares JV, Yu Y (2007) Distribution of aboveground live biomass in the Amazon basin. Glob Change Biol 13:816–837

Saatchi SS, Harris NL, Brown S, Lefsky M, Mitchard ETA, Salas W, Zutta BR, Buermann W, Lewis SL, Hagen S, Petrova S, White L, Silman M, Morel A (2011) Benchmark map of forest carbon stocks in tropical regions across three continents. Proc Natl Acad Sci USA 108:9899–9904

Schall P, Gossner MM, Heinrichs S, Fischer M, Boch S, Prati D, Jung K, Baumgartner V, Blaser S, Böhm S, Buscot F, Daniel R, Goldmann K, Kaiser K, Kahl T, Lange M, Müller J, Overmann J, Renner SC, Schulze ED, Sikorski J, Tschapka M, Türke M, Weisser WW, Wemheuer B, Wubet T, Ammer C (2018a) The impact of even-aged and uneven-aged forest management on regional biodiversity of multiple taxa in European beech forests. J Appl Ecol 55:267–278

Schall P, Schulze E-D, Fischer M, Ayasse M, Ammer C (2018b) Relations between forest management, stand structure and productivity across different types of Central European forests. Basic Appl Ecol 32:39–52

Shugart HH (2003) A theory of forest dynamics. The Blackburn Press, Caldwell

Shugart HH, Saatchi S, Hall FG (2010) Importance of structure and its measurement in quantifying function of forest ecosystems. J Geophys Res Biogeosci. https://doi.org/10.1029/2009JG000993

Shugart HH, Asner GP, Fischer R, Huth A, Knapp N, Le Toan T, Shuman JK (2015) Computer and remote-sensing infrastructure to enhance large-scale testing of individual-based forest models. Front Ecol Environ 13:503–511

Shugart HH, Wang B, Fischer R, Ma J, Fang J, Yan X, Huth A, Armstrong AH (2018) Gap models and their individual-based relatives in the assessment of the consequences of global change. Environ Res Lett 13:033001

Simard M, Pinto N, Fisher JB, Baccini A (2011) Mapping forest canopy height globally with spaceborne lidar. J Geophys Res Biogeosci 116:G04021

Snyder M (2010) What is forest stand structure and how is it measured? North Woodl 64:15

Stark SC, Leitold V, Wu JL, Hunter MO, de Castilho CV, Costa FRC, McMahon SM, Parker GG, Shimabukuro MT, Lefsky MA, Keller M, Alves LF, Schietti J, Shimabukuro YE, Brandao DO, Woodcock TK, Higuchi N, de Camargo PB, de Oliveira RC, Saleska SR (2012) Amazon forest carbon dynamics predicted by profiles of canopy leaf area and light environment. Ecol Lett 15:1406–1414

Tello M, Pardini M, Papathanassiou K, Fischer R (2014) Towards forest structure characteristics retrieval from SAR tomographic profiles. In: Electronic proceedings EUSAR 2014; 10th European conference on synthetic aperture radar, 03–05 June 2014, Berlin, Germany. VDE Verlag, Berlin, pp 1425–1428

Tello M, Cazcarra-Bes V, Fischer R, Papathanassiou K (2018) Multiscale forest structure estimation from SAR tomography. In: Electronic proceedings EUSAR 2018; 12th European conference on synthetic aperture radar, 04–07 June, 2018, Aachen, Germany. VDE Verlag, Berlin, pp 600–603

Tews J, Brose U, Grimm V, Tielbörger K, Wichmann MC, Schwager M, Jeltsch F (2004) Animal species diversity driven by habitat heterogeneity/diversity: the importance of keystone structures. J Biogeogr 31:79–92

Thuenen-Institut (2015) Dritte Bundeswaldinventur - Basisdaten (Stand 20.03.2015)

Wiegand T, He F, Hubbell SP (2013) A systematic comparison of summary characteristics for quantifying point patterns in ecology. Ecography 36:92–103

Young BD, D'Amato AW, Kern CC, Kastendick DN, Palik BJ (2017) Seven decades of change in forest structure and composition in *Pinus resinosa* forests in northern Minnesota, USA: comparing managed and unmanaged conditions. For Ecol Manag 395:92–103

Zenner EK, Hibbs DE (2000) A new method for modeling the heterogeneity of forest structure. For Ecol Manag 129:75–87

Affiliations

Rico Fischer[1] [iD] **· Nikolai Knapp[1] · Friedrich Bohn[1,2] · Herman H. Shugart[3] · Andreas Huth[1,4,5]**

✉   Rico Fischer
     rico.fischer@ufz.de

[1]   Department of Ecological Modeling, Helmholtz Centre for Environmental Research GmbH – UFZ, Permoserstasse 15, 04318 Leipzig, Germany

[2]   Institute for Meteorology and Climate Research, Atmospheric Environmental Research, Karlsruhe Institute of Technology, Kreuzeckbahnstrasse 19, 82467 Garmisch-Partenkirchen, Germany

[3]   Department of Environmental Sciences, University of Virginia, Charlottesville, VA 22903, USA

[4]   German Centre for Integrative Biodiversity Research (iDiv) Halle-Jena-Leipzig, Deutscher Platz 5e, 04103 Leipzig, Germany

[5]   Institute of Environmental Systems Research, University of Osnabrück, Barbarastr. 12, 49076 Osnabrück, Germany